Electronic Structure and Bonding in the Ternary Silicide $YNiSi_3$

Gi-Hong Sung and Dae-Bok Kang*

Department of Chemistry, Kyungsung University, Busan 608-736, Korea
Received November 27, 2002

An analysis of the electronic structure and bonding in the ternary silicide $YNiSi_3$ is made, using extended Hückel tight-binding calculations. The $YNiSi_3$ structure consists of Ni-capped Si_2 dimer layers and Si zigzag chains. Significant bonding interactions are present between the silicon atoms in the structure. The oxidation state formalism of $(Y^{3+})(Ni^0)(Si_3)^3$ for $YNiSi_3$ constitutes a good starting point to describe its electronic structure. Si atoms receive electrons from the most electropositive Y in $YNiSi_3$, and Ni 3d and Si 3p states dominate below the Fermi level. There is an interesting electron balance between the two Si and Ni sublattices. Since the π^* orbitals in the Si chain and the Ni d and s block levels are almost completely occupied, the charge balance for $YNiSi_3$ can be rewritten as $(Y^{3+})(Ni^{2-})(Si^{2-})(Si\text{-}Si)^+$, making the Si_2 layers oxidized. These results suggest that the Si zigzag chain contains single bonds and the Si_2 double layer possesses single bonds within a dimer with a partial double bond character. Strong Si-Si and Ni-Si bonding interactions are important for giving stability to the structure, while essentially no metal-metal bonding exists at all. The 2D metallic behavior of this compound is due to the Si-Si interaction leading to dispersion of the several Si_2 π bands crossing the Fermi level in the plane perpendicular to the crystallographic *b* axis.

Key Words : Band structure, Bonding, Silicide

Introduction

Metal silicides are valued for their hardness, chemical stability, and high melting point and are involved in applications such as high-temperature structural materials[1] and silicon technology.[2] Many ternary silicides are known, often containing a rare-earth metal or an early transition metal as one component and a late transition metal as another component.[3,4] For combinations of these metals, the vast majority of these compounds contain Ni.[5] Difficulties in the crystal growth of silicides often hinder their crystal structure determination and could limit proper characterization.

Recently Kanatzidis and co-workers reported the structure and properties of the two ternary silicides $MNiSi_3$ (M=Sm, Y) synthesized in Ga metal flux.[6] The structures, determined by single-crystal X-ray diffraction, adopt the $SmNiGe_3$ structure type[7] with zigzag Si chains and Si_2 dimers. $YNiSi_3$ crystallizes orthorhombic (space group *Cmmm*) with lattice constants of a = 3.930 Å, b = 21.021 Å, and c = 3.960 Å. The three-dimensional structure of $YNiSi_3$ is shown in Figure 1.

As one can see from the structural discussion in the next section, the simple Zintl concept is not applicable to this compound. According to the Zintl viewpoint, the electronegative Si atoms attain an octet on the Si chains (**1**) and the Si_2 dimers (**2**) through formation of covalent bonds or presence of lone pairs. The Si oxidation states in the chain and dimer units are regarded as -2 and -3, respectively. This would give eight negative formal charges per three silicons.

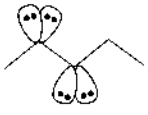

1

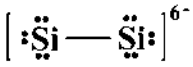

2

Therefore, if Y is in the oxidation state +3, the charge balance of $YNiSi_3$ can be written as $(Y^{3+})(Ni^{5-})(Si^{2-})(Si_2)^{6-}$. An unreasonably high oxidation state for Ni is not acceptable, because the Pauling electronegativities for Ni (1.8) and Si (1.8) are so similar that it is not likely that Ni is electropositive enough to donate electrons to Si. Obviously some electrons should be transferred from the Si anions to the empty d-block levels of the Ni^{5-} cation. If so, from which Si sublattice are the electrons removed? And what is the electronic configuration of the Ni and Si sublattices? In the present work, we examine these questions and the bonding characteristics by calculating the electronic structures of $YNiSi_3$ using the extended Hückel tight-binding (EHTB) method.[8,9] The atomic parameters employed for our calculations are listed in Table 1.

Crystal Structure

In order to understand our discussion of the electronic

Table 1. Atomic Parameters Used in the Calculations

atom	orbital	H_{ii} (eV)	ζ_1	C_1^a	ζ_2	C_2^a	ref
Y	5s	-6.01	1.74				14
	5p	-3.62	1.70				
	4d	-5.74	1.56	0.8213	3.55	0.3003	
Ni	4s	-9.0	2.10				15
	4p	-4.2	2.10				
	3d	-10.5	5.75	0.5683	2.00	0.6292	
Si	3s	-17.3	1.383				15
	3p	-9.2	1.383				

[a]Coefficients in double-ζ expansion.

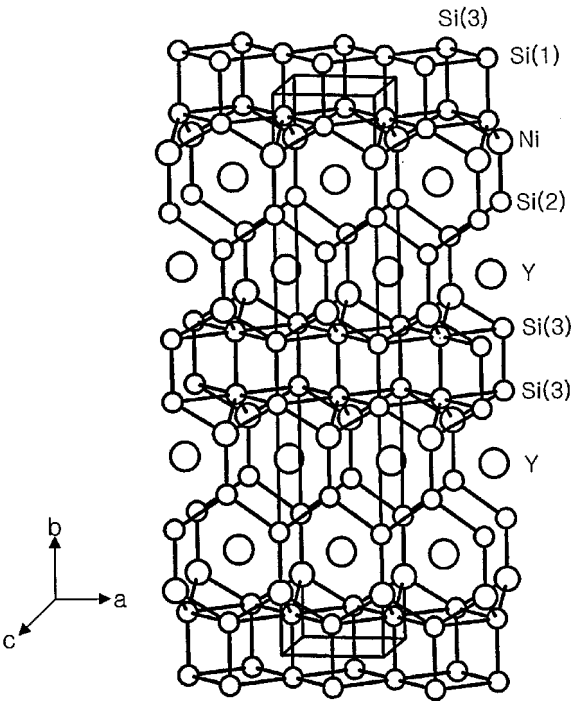

Figure 1. Crystal structure of $YNiSi_3$ with the unit cell outlined.

structure of $YNiSi_3$, it is necessary to describe its crystal structure briefly. $YNiSi_3$ contains pseudo-hexagonal nets formed by Si and Ni atoms in the *ab* plane (see Figure 1). There are two different types of silicon fragments, infinite zigzag Si chain and Si_2 dimer layer. In the former case, each Si has two Si neighbors at a distance of 2.386 Å, forming infinite kinked Si chains. The Si chains run along the *a* axis with the plane of the chain being parallel to the *ab* plane. The arrangement of the latter Si atoms may be viewed as a two-dimensional (2D) array of Si pairs, aligned parallel to the *b* axis. The Si-Si distance within the dimers is 2.35 Å and is essentially identical to that in elemental Si.[10] The closest Si-Si contacts between adjacent dimers are very short (2.79 Å) compared to the van der Waals distance (4.2 Å) between two silicon atoms.[11] The double layers of Si chains and Si dimers are connected via a layer of Ni atoms, which are coordinated in a slightly distorted square pyramidal geometry to two Si(1) atoms at 2.29 Å and two Si(3) atoms at 2.27 Å forming the base, and to a Si(2) atom at 2.26 Å forming the apex. This produces a 3D pseudo-hexagonal tunnel framework with Y atoms filling the tunnels. Thus the primary Si-Si separations in chains and dimers, 2.386 and 2.35 Å, are clearly bonding contacts and the 2.79 Å separation between pairs in the 2D layer is also most probably bonding. The observed Ni-Si distances compare favorably to the Pauling single bond distance of 2.33 Å. The short distances may imply a significant bonding interaction between them.

Electronic Structure

A. Oxidation State of $YNiSi_3$. An interesting issue here is how the valence electrons are distributed in this compound. At first glance, the electronic distribution in $YNiSi_3$ seems to

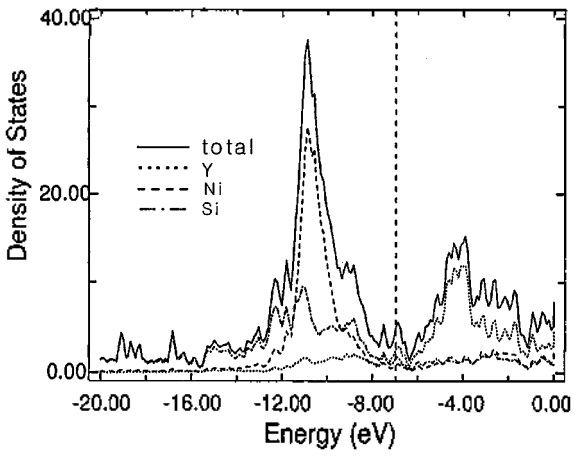

Figure 2. Density of states (DOS) plots for $YNiSi_3$ and its Y, Ni, and Si projections. The Fermi level is drawn in the dashed line at -6.96 eV.

be straightforward. The assumption that the formal charge of Y would be 3+ is reasonable, because it is the most electropositive atom in $YNiSi_3$. This is also supported by the projected DOS curves in Figure 2 which shows contributions of the Y, Ni, and Si atoms to the total density of states (DOS) calculated for $YNiSi_3$. The projected DOS curves reveal substantial covalent mixing of these states. Above the Fermi level (E_f), the unfilled states have their major contribution from Y 4d orbitals, so Y transfers all its valence electrons to become Y^{3+}. Therefore, we can assign the electron distribution as Y^{3+} $[NiSi_3]^{3-}$. Since Ni is as electronegative as Si, however, it is not likely that Ni will donate electrons to silicons. The narrow peak from -9.5 to -11.5 eV located well below the Fermi level represents filled states composed mainly of Ni 3d character. With all its 3d orbitals fully occupied, it would appear that Ni has a configuration of d^{10} and is either neutral (Ni^0) or possibly even negatively charged (Ni^{2-}), consistent with the absence of any measurable moment on Ni.[6] This could be responsible for the relatively short Y-Ni distance of 3.05 Å. If we assume a d^{10} configuration for the Ni atoms, we arrive at the formulation $[Y^{3+}Ni^0(Si_3)^{3-}]$. The oxidation state $(Si_3)^{3-}$ can be rewritten as $(Si^-)(Si_2)^{2-}$ or $(Si^{2-})(Si_2)^-$, which implies that what to assign as a formal charge for the isolated sublattices, the zigzag Si chain and the 2D Si_2 layer, is not obvious. These observations suggest that the conventional electron counting scheme fails to give a realistic picture in cases such as these. To further address this problem, we need to take a closer look at the bonding characteristics of this silicide by simply assigning one negative charge to each Si, even though there is a common Fermi level in the full lattice.

B. The Si Chain. One type of Si that is present in the structure forms zigzag chains with Si-Si distances of 2.386 Å, well separated from neighboring Si chains. The band structure of the infinite Si chain is shown in Figure 3a. The bands are labeled as σ or π. The essential bonding is that of the familiar polyacetylene chain.[12] All energy bands are folded back at the zone boundary, X,[12] as a consequence of the 2-fold screw axis symmetry of the chain with the Si_2 unit cell. There are two low-lying σ (σ_1, σ_2) bands, both Si-Si

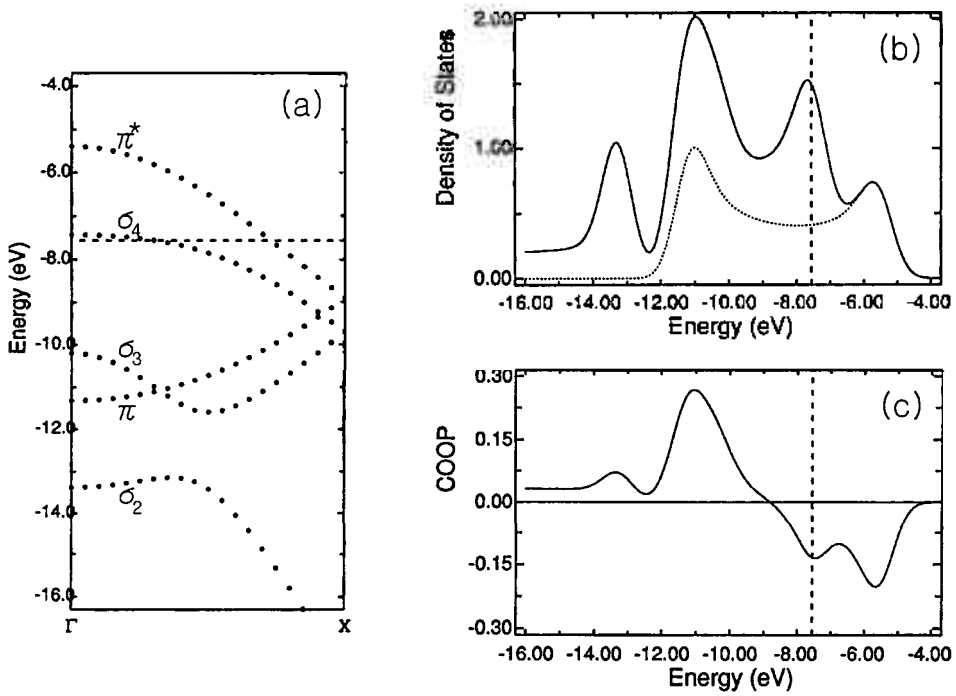

Figure 3. (a) Band structure, (b) DOS, and (c) COOP of a one-dimensional zigzag Si chain. In part b the dotted line corresponds to the projection of the Si π orbitals. In part c the solid line corresponds to the Si-Si COOP. The Fermi level is drawn in the dashed line for 10 e^-, *i.e.*, Si_2^{2-}.

bonding, the upper one less so. The two branches of the band are labeled as π and π^*. The π and π^* (p_z) bands are in the same energy range as the bonding σ_3 and σ_4 (p_x and p_y) levels. Here, the x, y, and z axes correspond respectively to the *a*, *b*, and *c* crystallographic directions for the coordinate system given in Figure 1. The top of the π^* band is Si-Si antibonding and the bottom of it is nonbonding; while the top of the π band is nonbonding and the bottom of it is Si-Si bonding. The antibonding σ^* (σ_5, σ_6) levels are at higher energies (not shown in the figure). The DOS plots of these bands are shown in Figure 3b. The bonding and antibonding character of the bands can be seen in the crystal orbital overlap population (COOP)[9] curves presented in Figure 3c.

If we assume five electrons per Si for the purposes of the present discussion, a canonical form of the resonance structure for the $_\infty^1[Si_2^{2-}]$ zigzag chain would be described schematically as **3**. As we fill all bonding levels with 10 electrons per Si_2 unit cell, the highest occupied π (p_z) band

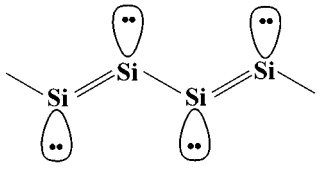

3

contains two electrons. Due to the way the σ_4 and π bands cross, however, the σ_4 band is incompletely filled and the π^* band is slightly occupied (see Figure 3a). The integrated overlap population for the Si-Si bond is calculated to be 0.97. We are now in a position to discuss the Si chains enveloped by the Ni double layer. In this chain each Si is connected to the nickel atoms, as indicated by **4**. For those silicon atoms connected to Ni, there are two types of orbitals

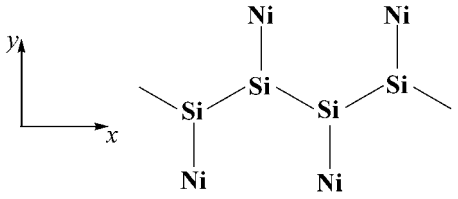

4

that are responsible for the Ni-Si interactions. One of them, likely to interact more strongly with the nickel, is the σ-type orbital illustrated in **5** at left, and the other is a π-type orbital shown in **5** at right. These orbitals interact with the appropriate symmetry-adapted orbitals on nickel.

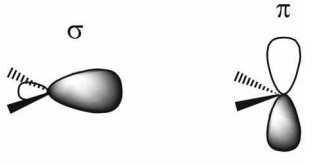

5

The calculated band structure of this one-dimensional sublattice (**4**) is shown in Figure 4c. To see how the Si-Ni interactions occur we also show the band structures of a zigzag $(Si_2^{2-})_\infty$ chain without the nickel atoms (Figure 4a)

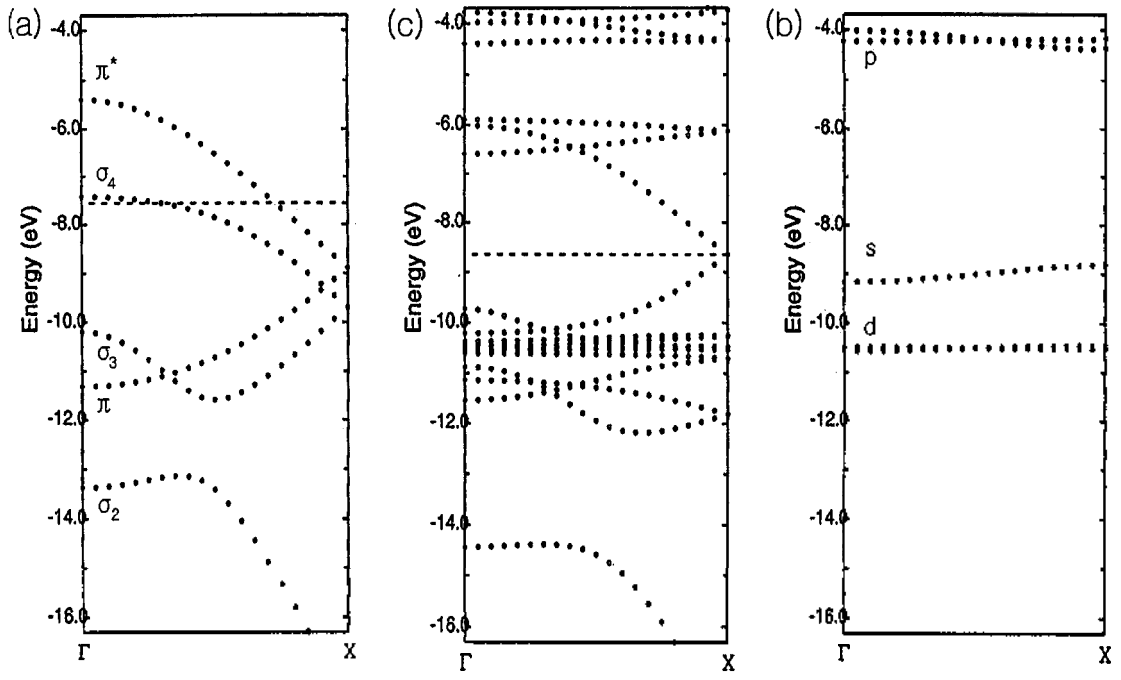

Figure 4. Band structures for (a) the zigzag silicon sublattice, (b) the nickel sublattice, and (c) the composite structure of a one-dimensional zigzag Si chain enveloped by Ni atoms, *i.e.*, $(Ni_2Si_2^{2-})_\infty$. The dashed line marks the Fermi level.

and two linear $(Ni^0)_\infty$ needles (Figure 4b). In the band structure for the nickel sublattice (Figure 4b), the different dispersion of the d bands results from the different extent of overlap of the five d orbitals with those in the neighboring cells. The $d_{x^2-y^2}$ band has the largest dispersion, due to the relatively strong σ overlap. The degenerate π bands (d_{xy} and d_{xz}) are flatter because of π smaller overlap between d orbitals. Due to very small overlap between δ orbitals, the d_{yz} and d_{z^2} bands are really quite flat. In fact, all these bands are almost dispersionless because of the large Ni-Ni separation in the sublattice. For an electron count of d^{10}, there are ten electrons to be placed in the five Ni d bands, making these d bands completely filled.

When the Si-Ni interactions are turned on, we note that there are considerable changes in the bands around the Fermi level (compare Figure 4c with Figure 4a). The important σ-type interaction takes place between the p_y bands (σ_2 at Γ, σ_3 and σ_4) of silicon and the Ni $d_{x^2-y^2}$ bands. This interaction is favored by the good energy match and the favorable overlap between these band orbitals. It results in the Si-Ni σ bonding (the bands around -14.5 and -11.5 eV in Figure 4c) and the Si-Ni σ^* antibonding bands (narrow ones around -6.0 eV in Figure 4c), which are shifted down and up, respectively, relative to the σ_2 at Γ, σ_3 and σ_4 bands of the pure Si chain. The orbital mixing just described is nicely shown in the DOS projections of the silicon p_y and nickel $d_{x^2-y^2}$ orbitals in Figure 5. The COOP curve for the Si-Ni bond also present in Figure 5 shows the bonding and antibonding character of these bands. The gap between the two bonding peaks at -14.5 and -11.5 eV is due to the avoided crossing. The lack of Si-Ni antibonding character in the -6.0 eV region can be explained by the mixing of higher-lying Ni $4p_y$ orbital into the antibonding combination in a Si-Ni bonding way. The silicon π and π^* (or p_z) bands are also rearranged due to their π interaction with the nickel d_{yz} bands. These bands extending between -10.2 and -6.0 eV are slightly destabilized, a consequence of the Si-Ni π antibonding interaction; compare the half-filled π band in Figure 4c with the π band in Figure 4a. The bonding counterpart bands of the Si-Ni π interaction are in the bonding zone localized between -11.5 and -10.6 eV.

To align the Fermi levels in both silicon and nickel chain substructures, some electron density flows from silicon to nickel sublattices. The Fermi level for the $Ni_2Si_2^{2-}$ chain is thus lowered slightly relative to the pure Si chain. The calculated average overlap populations (OP) for the $Ni_2Si_2^{2-}$ chain are 0.72 for the Si-Ni bonds and 0.98 for the Si-Si bonds, respectively. A comparison with the OP in $(Si_2^{2-})_\infty$ zigzag chain (Si-Si OP=0.97) suggests that the Si-Si bonding in the $Ni_2Si_2^{2-}$ chain is slightly strengthened as compared to that in $(Si_2^{2-})_\infty$. The COOP curve (Figure 5) confirms this expectation. In the COOP plots we see that the originally partially filled π^* band just below the Fermi level in Figure 3 is left unoccupied in $(Ni_2Si_2^{2-})_\infty$.

C. The Si_2 Layer. Two Si atoms in the $YNiSi_3$ structure form dimers that are collinear with the *b* axis direction and are arranged side by side in a rectangular array which extends over the *ac* plane (Figure 1). There are two slightly different types of dimers [Si(1)-Si(1) and Si(3)-Si(3)] in Si-Si separations. They are 2.346 and 2.350 Å, respectively, and the Si-Si distances between adjacent dimers are 2.789 Å.

Let us first consider the idealized square Si_2 layer, adapted from the $YNiSi_3$ structure. For the construction of the band structure of the two-dimensional double layer, we use both

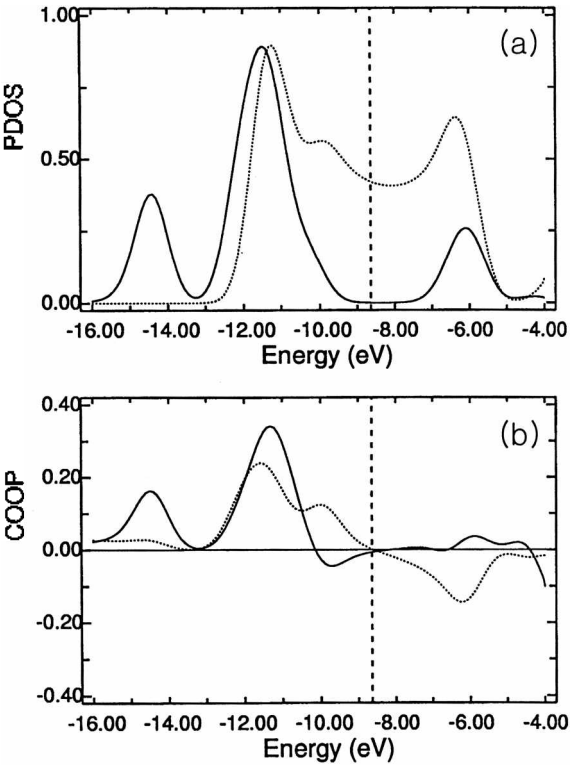

Figure 5. (a) Projected DOS and (b) COOP plots of a one-dimensional zigzag Si chain enveloped by Ni atoms, *i.e.*, $(NiSi_2^{2-})_\infty$. The p_y (σ) and p_z (π) orbitals of Si are projected out in the DOS as solid and dotted lines, respectively. COOP plots illustrate the Si-Ni (solid line) and Si-Si (dotted line) bonding character of the bands. The dashed line marks the Fermi level.

primitive (small) and centered (large) square cells. The transition to the latter lattice can be accomplished by folding the band structure of the former lattice.

The detailed analysis of the folding-back procedure has been given elsewhere[12] and will not be repeated here. A two-dimer cell is taken here because the large lattice is present in the structure of $YNiSi_3$. The resultant band structure has twice as many bands in every direction, as shown in Figure 6b. The band structure of the small lattice (Figure 6a) contains the lowest σ_s band and two lone pair combinations (n_+, n_-) lying higher in energy, a result of strong s, p_y orbital mixing. Above the two lone pair bands we have two π pair bands that are bonding and antibonding within the dimer and the highest σ_p^* level. The corresponding DOS and COOP curves are shown in Figure 7. An examination of the COOP curves shows that maximum bonding for the Si-Si bonds between dimers and within the dimers is achieved with different electron counts. With eight electrons (per Si_2 unit) all bonding states within the dimers are filled and anti-bonding states are slightly occupied. A similar situation occurs for the bonds between dimers with nine electrons. It can also be seen from the COOP curves in Figure 7 that ten electrons per Si_2 would be an unreasonably high electron count for the double layer since both bonds are weakened. In the layer the maximal intrapair bonding occurs for electron counts lower than 10. This is a consequence of some intrapair π^* bands coming to low energy as a result of bonding interpair interactions. For an electron count of 8 per Si_2 we occupy the σ and π bands that are mainly bonding with respect to the dimer and the layer. The Si-Si overlap populations for this electron count are 0.90 and 0.41 within and between the dimers, respectively. With one additional electron the corresponding overlap populations are 0.85 and 0.42. Consequently, the Si-Si interpair bonding in the layers remains nearly unchanged, while the Si-Si bonding in the dimers is slightly weakened because of filling of π^* antibonding states.

We now want to take a look at the influence of the Ni

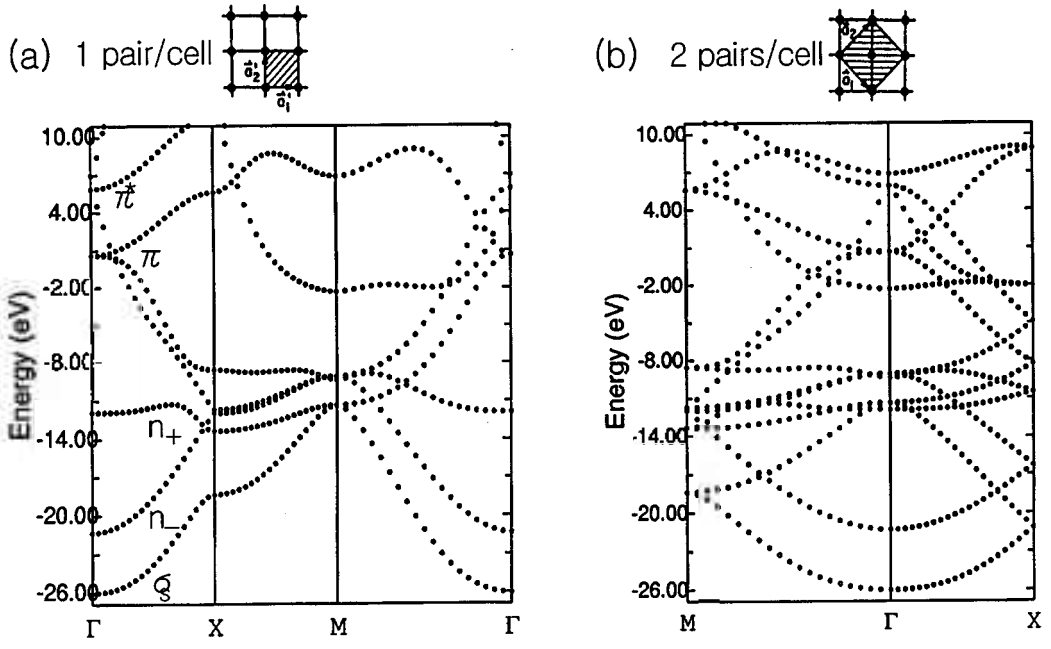

Figure 6. Band structure of a square layer of Si_2 dimers: (a) with a primitive cell and (b) after the back-folding process. The unit cell is outlined at top of each plot.

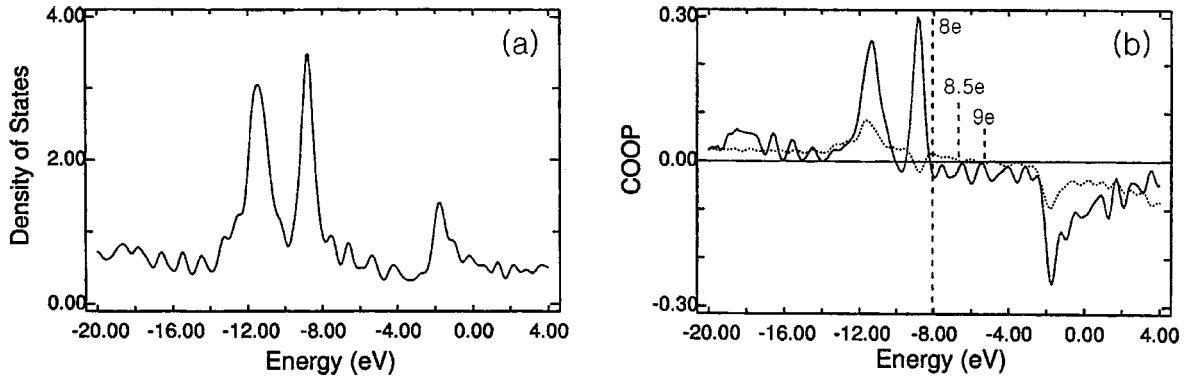

Figure 7. (a) DOS and (b) COOP plots of a square layer of Si_2 dimers. In the COOP plots the Si-Si bonds between dimers and within the dimers are drawn in the dotted and solid lines, respectively. The Fermi levels for different electron populations are shown as dashed lines in the COOP.

atoms capping the Si_2 layer from above and below in the real structure. When the Ni atoms are considered, the bands can mix appreciably. Some low-lying Si bands are stabilized in energy as a result of bonding interactions with Ni atoms. The band structure in Figure 8 manifests traces of the band structure for the large cell of the double layer (Figure 6b). The Si atoms in the layer were tentatively considered as Si^-. The large cell contains two Si_2 molecules and two Ni atoms, with their orbitals filled by 40 electrons. This leads to an occupation of antibonding intrapair Si-Si states (Figure 8c) below the Fermi level, which, however, optimizes Si-Ni bonding (Si-Ni OP = 0.41). It should be noted that the Fermi level (-5.36 eV) of this $NiSi_2^{2-}$ layer is substantially higher than that (-8.65 eV) of the $Ni_2Si_2^{2-}$ chain.

D. The Full $YNiSi_3$ Structure. The two Si substructures in $YNiSi_3$ are well separated from each other and do not interact directly. Therefore, the DOS contributions of the separately calculated Si sublattices, namely a chain (Figure 9c) and a layer (Figure 9b) of Si atoms surrounded by their Ni neighbors, are consistent with the projected DOS of Si atoms calculated for the full $YNiSi_3$ structure (Figure 9a). Si atoms provide the majority of their states below the Fermi level. The DOS curve (Figure 2) shows that although most of the Y 4d states are above the Fermi level, a small portion is found to be mixing with Ni 3d and Si 3p states in bonding levels below the Fermi level. Initially all bonding energy

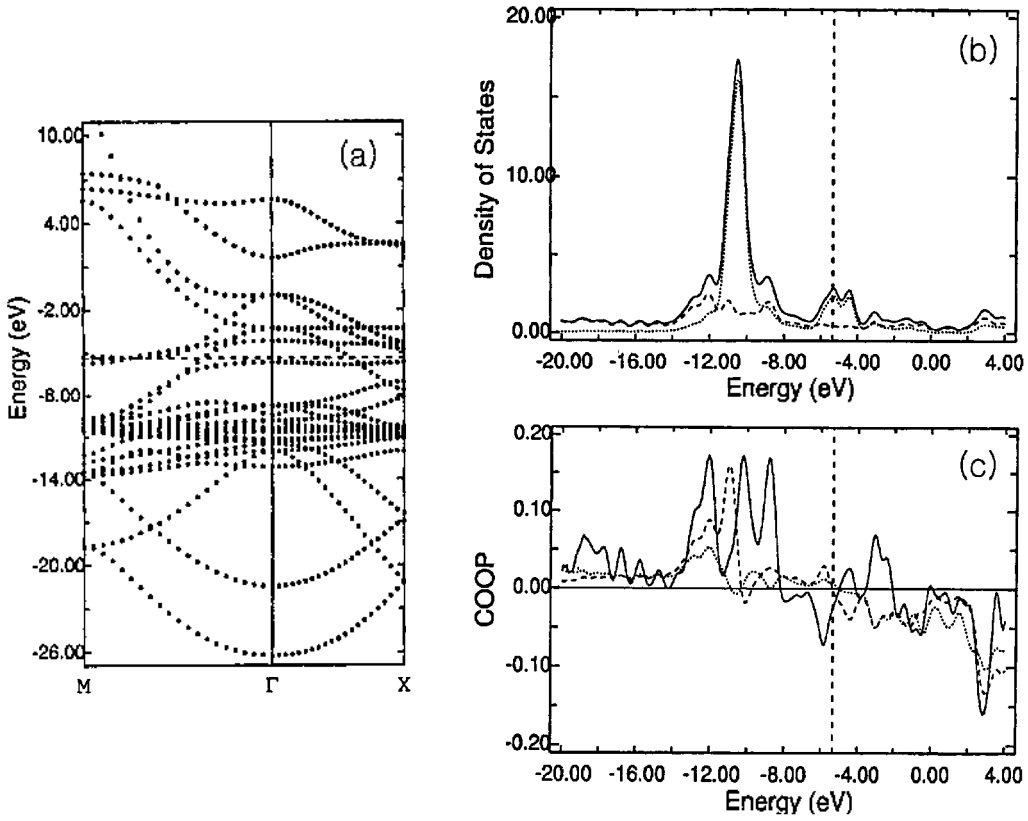

Figure 8. (a) Band structure, (b) DOS and (c) COOP of a $NiSi_2$ layer. Contributions of Si (dashed line) and Ni (dotted line) to the total DOS (solid line) are shown in the DOS. The Fermi level is marked for $2NiSi_2^{2-}$. In part c the Si-Si overlap populations are shown as solid lines within the dimers, and as dotted lines between dimers. The Si-Ni bonding (dashed line) is optimized with all bonding levels and no antibonding levels occupied at the Fermi level.

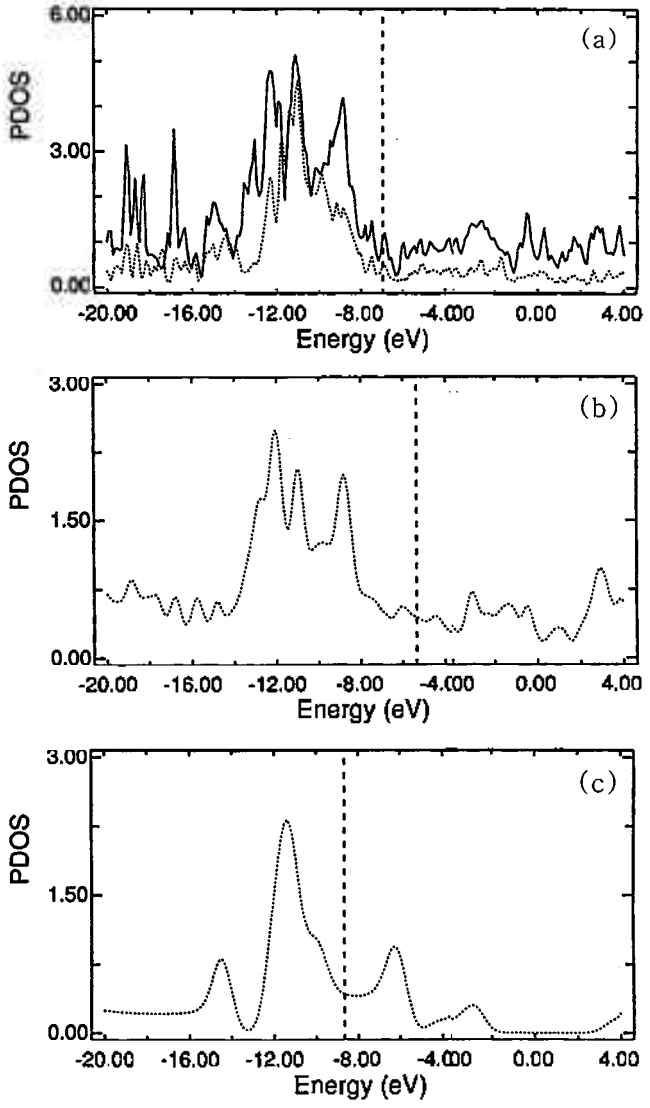

Figure 9. (a) Contributions of Si_2 layers (solid line) and Si chains (dotted line) to the total DOS of $YNiSi_3$, and the projected DOS of Si atoms calculated for (b) the layers and (c) the chains surrounded by their Ni neighbors. The dashed line refers to the Fermi level.

states of the Si chain were filled with five electrons per Si. As we saw, Si-Si antibonding π^* states of the Si_2 layer are occupied for the unreasonably high-lying 10-electron Fermi level of the layer. In the complete structure, therefore, some electrons are shifted from the Si_2 layers to the rest of the structure. According to the modified electron counting scheme,[13] three electrons should be transferred from the $(Si\text{-}Si)^{2-}$ layer to fill the π^* orbitals in the Si chain and the Ni d- and s-block levels. With the Fermi level at -6.96 eV, a consequence of equalization of the Fermi levels of the component sublattices, the antibonding π^* states of the Si chain become occupied, as shown in Figure 10. At the Fermi level, a substantial part of the Ni s and p bands is occupied, so that the calculated Ni configuration is $d^{9.52}s^{0.49}p^{0.85}$. An electron occupation picture of the two Si and Ni substructures after such an electron transfer is illustrated schematically by **6**.

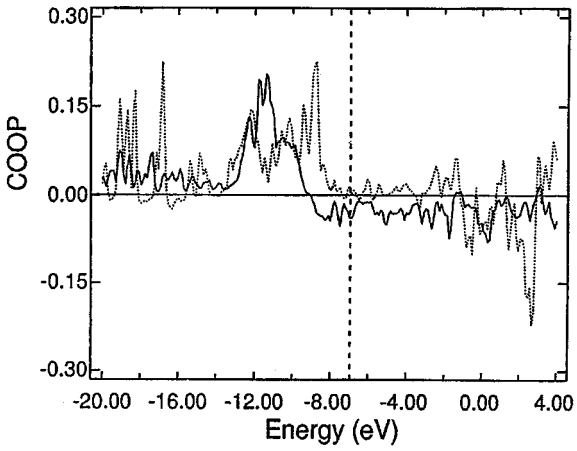

Figure 10. COOP curves of the Si-Si bonds: (a) in the one-dimensional Si chains (solid line), (b) within the dimers in the Si_2 layers (dotted line) calculated for the three-dimensional $YNiSi_3$ structure. The dashed line refers to the Fermi level.

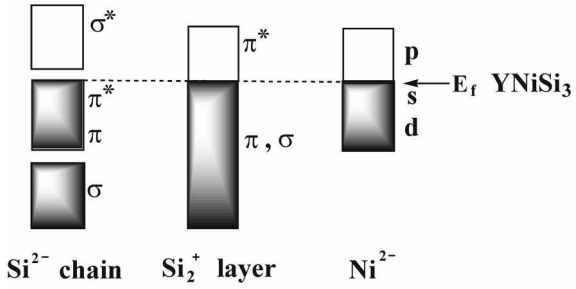

6

This makes the Si chain and Ni atoms formally Si^{2-} and Ni^{2-}, respectively. Only seven electrons are formally present in the Si_2 layer, making it a Si_2^+ double layer. The resulting Si-Si overlap populations calculated for the full $YNiSi_3$ structure are 0.81 for Si atoms forming the chains (Si-Si distance 2.386 Å). Relatively large overlap populations within the Si dimers (Si-Si = 2.35 Å) of 0.86 are the result of a two-center two-electron bond strengthened by π bonding interactions.

Consistent with all these expectations, the calculated charge distribution is $Y^{1.20}Ni^{0.86-}Si^{0.51-}(Si_2)^{0.17-}$. The Si atoms forming the dimers seem to be slightly oxidized. On the contrary, the Ni and the Si atoms forming zigzag chain are best thought of as being reduced. While we do not place much emphasis on the calculated numbers, qualitatively the distribution of electron density seems plausible. There is, of course, substantial orbital mixing of Y states. Bonding within $YNiSi_3$ is highly covalent and both Si-Ni and Si-Si interactions provide the major source of its stability. The integrated overlap populations were determined for various contacts in $YNiSi_3$ to gauge the strength of these interactions and are listed in Table 2. As shown in the COOP, the Si-Ni bonding levels are nearly filled up to the Fermi level even though there are some bonding levels of it above the Fermi level (Figure 11).

The band structure of $YNiSi_3$ is shown in Figure 12. The

Table 2. Selected Interatomic Distances (Å) and Overlap Populations (OP) for $YNiSi_3$

	distances (Å)	OP
Y - Ni	3.048	0.08
Y - Si(2)	2.975	0.20
Ni - Si(2)	2.262	0.49
Ni - Si(3)	2.272	0.31
Si(1) - Si(1)	2.346	0.87
Si(2) - Si(2)	2.386	0.81
Si(1) - Si(3)	2.789	0.33

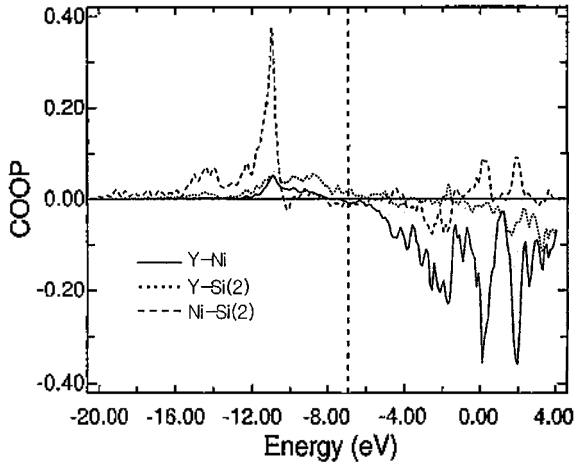

Figure 11. COOP curves for the Y-Ni, Y-Si(2), and Ni-Si(2) contacts in $YNiSi_3$. The Fermi level is drawn in the dashed line at -6.96 eV.

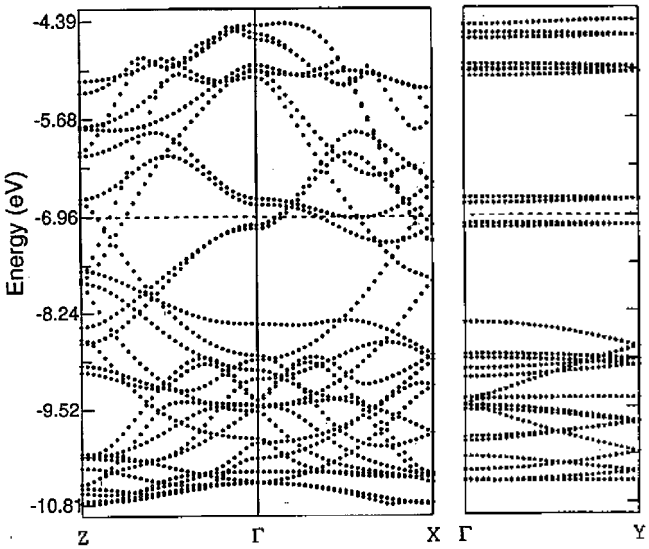

Figure 12. Band structure of $YNiSi_3$ (the dashed line indicates the Fermi level). $\Gamma = (0, 0, 0)$, $X = (a^*/2, 0, 0)$, $Y = (0, b^*/2, 0)$, and $Z = (0, 0, c^*/2)$.

Fermi level crosses significantly dispersive bands along the lines $\Gamma \rightarrow X$ and $\Gamma \rightarrow Z$ corresponding to the a and c directions in the crystal, respectively. The band dispersion along the line $\Gamma \rightarrow Y$, which corresponds to the b direction in the crystal, is very small. These results suggest the importance of Si-Si bonding interactions in the Si chains and layers parallel to the axial directions of the ac plane of the structure. The metallic conductivity is thus predicted to be a two-dimensional (2D) metal. The π and π^* bands of these sublattices are responsible for the expected electronic conductivity of $YNiSi_3$ (see the Figure 9a showing the significant contributions of Si_2 layers to the total DOS near the Fermi level). The greater number of bands crossed along ΓX than along ΓZ may result in the better conduction along the crystallographic a direction.

Conclusions

The $YNiSi_3$ structure consists of Ni-capped Si_2 dimer layers and Si zigzag chains. Ni and Si atoms receive electrons from the most electropositive Y in $YNiSi_3$, and hence Ni 3d, 4s, and Si 3p states dominate below the Fermi level. Since the π^* orbitals in the Si chain and the Ni d and s block levels are almost completely occupied, the charge balance for $YNiSi_3$ can be written as $(Y^{3+})(Ni^{2-})(Si^{2-})(Si\text{-}Si)^{1-}$, making the Si_2 layers oxidized. These results suggest that the Si zigzag chain contains single bonds and the Si_2 double layer possesses single bonds within a dimer with a partial double bond character. Strong Si-Si and Ni-Si bonding interactions are important for giving stability to the structure, while essentially no metal-metal bonding exists at all. The 2D metallic behavior of this compound is due to the Si-Si interaction leading to dispersion of the several Si_2 π bands crossing the Fermi level in the plane perpendicular to the crystallographic b axis.

References

1. Shah, D. M.; Berczik, D.; Anton, D. L.; Hecht, R. *Mater. Sci. Eng. A* **1992**, *155*, 45.
2. Reader, A. H.; Vanommen, A. H.; Weijs, P. J. W.; Wolters, R. A. M.; Oostra, D. J. *Rep. Prog. Phys.* **1993**, *56*(11), 1397.
3. Parthe, E.; Chabot, B. In *Handbook on the Physics and Chemistry of Rare Earths*; Gschneidner, K. A., Jr., Eyring, L., Eds.; Elsevier: Amsterdam, 1984; Vol. 6, p 113.
4. Villars, P. *Pearson's Handbook, Desk Edition*; ASM International: Materials Park, OH, 1997.
5. (a) TiNiSi: Shoemaker, C. B.; Shoemaker, D. P. *Acta Crystallogr.* **1965**, *18*, 900. (b) ZrNiSi, $ZrNi_2Si_2$, $HfNi_2Si_2$: Voroshilov, Yu. V.; Markiv, V. Ya.; Gladyshevskii, E. I. *Inorg. Mater. (Engl. Transl.)* **1967**, *3*, 1224. (c) HfNiSi: Ganglberger, E.; Nowotny, H.; Benesovsky, F. *Monatsh. Chem.* **1967**, *98*, 95. (d) $TiNiSi_2$, $HfNiSi_2$: Markiv, V. Ya.; Gladyshevskii, E. I.; Skolozdra, R. V.; Kripyakevich, P. I. *Dopov. Akad. Nauk. Ukr. RSR, Ser. A: Fiz.-Tekh. Mat. Nauki* **1967**, *3*, 266. (e) Ti_5Ni_3Si: Bardos, D. I.; Gupta, K. P.; Beck, P. A. *Trans. Metall. Soc. AIME* **1961**, *221*, 1087. (f) Zr_5Ni_3Si, Hf_5Ni_3Si: Mittal, R. C.; Si, S. K.; Gupta, K. P. *J. Less-Common Met.* **1978**, *60*, 75. (g) $Hf_3Ni_2Si_3$: Yarmolyuk, Ya. P.; Grin, Yu. N.; Gladyshevskii, E. I. *Sov. Phys. Crystallogr. (Engl. Transl.)* **1977**, *22*, 416. (h) $Zr_2Ni_3Si_4$, $Hf_2Ni_3Si_4$: Yarmolyuk, Ya. P.; Pecharskii, V. K.; Aksel'rud, L. G. *Sov. Phys. Crystallogr. (Engl. Transl.)* **1988**, *33*, 601. (i) $Ti_4Ni_4Si_7$: Horache, E.; Feist, T. P.; Stuart, J. A.; Fischer, J. E. *J. Mater. Res.* **1990**, *5*, 1887. (j) $Zr_5Ni\text{-}Si_{18}$, $Hf_5Ni_9Si_{16}$: Aksel'rud, L. G.; Lysenko, L. A.; Yarmolyuk, Ya. P.; Gladyslevskii, E. I. *Dopov. Akad. Nauk. Ukr. RSR, Ser. A: Fiz.-Mat. Tekh. Nauki* **1977**, *39*, 657. (k) $Ti_6Ni_{16}Si_7$, $Zr_6Ni_{16}Si_7$: Spiegel, F. X.; Bardos, D.; Beck, P. A. *Trans. Metall.*

Soc. AIME **1963**, *227*, 575. (f) $Hf_6Ni_{16}Si_7$: Gladyshevskii, E. I. *Sov. Powder Metall. Met. Ceram. (Engl. Transl.)* **1962**, *1*, 262.
6. Chen, X. Z.; Larson, P.; Sportouch, S.; Brazis, P.; Mahanti, S. D.; Kannewurf, C. R.; Kanatzidis, M. G. *Chem. Mater.* **1999**, *11*, 75.
7. Bodak, O. I.; Pecharskii, V. K.; Mruz, O. Ya.; Zavodnik, V. E.; Vilvitsava, G. M.; Salamanko P. S. *Dopov. Akad. Nauk. Ukr. RSR, Ser. B* **1985**, *2*, 37.
8. Whangbo, M.-H.; Hoffmann, R. *J. Am. Chem. Soc.* **1978**, *100*, 6093.
9. Hoffmann, R. *Solids and Surfaces: A Chemist's View of Bonding in Extended Structures*; VCH Publishers: New York, 1988.
10. Donohue, J. *The Structures of the Elements*; Wiley: New York, 1974.
11. Bondi, A. *J. Phys. Chem.* **1964**, *68*, 441.
12. Hoffmann, R.; Janiak, C.; Kollmar, C. *Macromolecules* **1991**, *24*, 3725 and references therein.
13. Lee, K.-S.; Koo, H.-J.; Dai, D.; Ren, J.; Whangbo, M.-H. *Inorg. Chem.* **1999**, *38*, 340.
14. Vlassov, M.; Palacin, M. R.; Beltran-Porter, D.; Oro-Sole, J.; Canadell, E.; Alemany, P.; Fuertes, A. *Inorg. Chem.* **1999**, *38*, 4530.
15. Landrum, G. A.; Hoffmann, R.; Evers, J.; Boysen, H. *Inorg. Chem.* **1998**, *37*, 5754.